3283

AIAA 2001-~~6040~~

Use of Dilatation in Understanding Composite Propellant Aging

D. D. Davis
Allitant Techsystems
Magna, Utah

37th AIAA/ASME/SAE/ASEE Joint Propulsion Conference and Exhibit
8-11 July 2001
Salt Lake City, Utah

AIAA-2001-6040

Use of Dilatation in Understanding Composite Propellant Aging

Deborah Davis
Alliant Techsystems
Magna, UT 84047

SUMMARY

This paper discusses the mechanical aging behavior of composite propellant, with an emphasis on surface aging. The propellant studied was a typical polybutadiene formulation, using an epoxy/amine bonding agent system. Results show the propellant ages through a combination of oxidative hardening and hydrolysis. A mechanistic description of propellant aging has been developed, using volume dilatation to determine the role of water in the observed aging. The nature of the oxidative hardening and hydrolytic attack suggest that stress and modulus can be best described using a parallel process kinetic model, while a simple first order model is a good approximation for strain aging. Available subscale aging data have been fit using those kinetic models, and Arrhenius plots of the resulting rate constants constructed. In addition, ambient aging model curves have been compared to full-scale motor plug data. The models tend to over-predict bulk propellant aging, but fit near-surface propellant aging reasonably well.

INTRODUCTION

Previous studies of composite propellant aging have shown evidence of two competing reactions involved in the overall aging behavior – oxidative hardening and hydrolysis. Modulus and stress initially increase with age, and then as hydrolysis catches up, modulus and stress begin to decrease. The observed aging behavior has been modeled in the past using a parallel process kinetic model.

Figure 1 shows an idealized sketch of propellant, with one side exposed to air. The propellant can be separated into three aging 'layers'; an as-cast, binder rich layer, a thin surface layer, and the remaining bulk propellant. The binder-rich, as-cast layer is not important structurally or ballistically, but is important as a boundary layer for diffusion processes. The current aging study discussed below ignores diffusion processes, and concentrates on the remaining two propellant zones underneath.

Underneath the as-cast layer is a thin surface layer. This layer ages faster than bulk propellant. Plugs taken from full-scale motors have a tough 'skin' on the bore surface of the propellant. Previous aging studies generally show a surface aging zone about 0.1" thick[1].

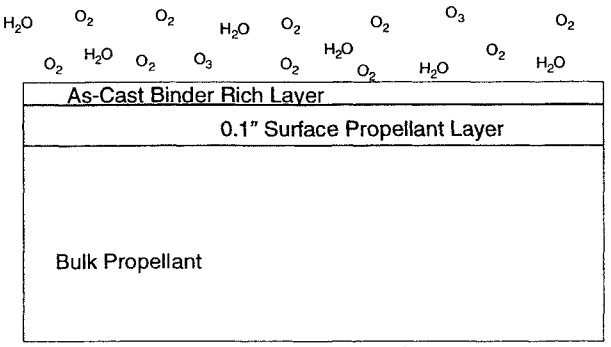

Figure 1. Propellant Diagram

In terms of aging, it is important to note that surface propellant and bulk propellant are chemically identical. They contain the same ingredients, and at the same rough concentrations. The primary difference between this surface layer and the bulk most likely involves subtle differences in solid particle size distribution, common at interfaces.

The chemical similarity between surface and bulk propellant implies that the two regions age via the same mechanisms, in this case oxidative hardening and hydrolysis. The difference in aging behavior then, is a result of the difference in aging rates. Surface aging occurs at a faster rate than bulk, due to the higher concentration of air and water at the surface, as compared to bulk propellant. There is also evidence that the surface layer 'seals' during aging, providing a progressively more effective barrier. Diffusion through the layer slows as a result of aging[2].

The mechanical property data generated under previous studies have been fit using a parallel process kinetic model[3,4], shown below:

$$P(t) = (F \times P_0)\,[k_1/(k_2-k_1)]\,(e^{-k1t} - e^{-k2t}) + (P_0\, e^{-k2t})$$

Where

$P(t)$, P_0 = property at time t, zero-time
F = proportionality constant
k_1, k_2 = rate constants.

This model assumes two competing first order reactions:

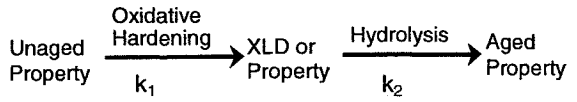

Oxidative hardening is well known in composite propellant aging. It is known to involve the double bonds of the polymer backbone, and in fact, anti-oxidants are commonly added to propellant formulations to limit the effect.

The role of hydrolysis in composite propellant aging is not understood, however. The effect of moisture during aging is subtle, and is not always easy to distinguish over the larger relative effect of oxidative hardening. The study described below was designed to improve that understanding, both in terms of the overall kinetic behavior, and in terms of general mechanism.

APPROACH

The formulation used in this study was a typical composite propellant, using an HTPB/isocyanate polymer system, 88% AP/Al solids, and an epoxy/amine bonding agent. Propellant from four full-scale mixes was obtained and cast into buckets. The cured 8 inch diameter propellant slugs were prepared for aging by first cutting them into quarters, then slicing each quarter into ½" slices, as shown in Figure 2.

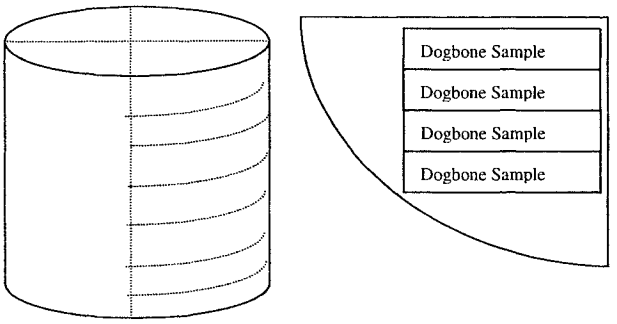

Figure 2. Aging Sample Configuration

Each slice was randomly assigned to one of five different groups. Each group was preconditioned for 4 weeks at 77°F, and at one of the following humidities; 0, 5, 10, 15, and 25%RH. Relative humidity was controlled using water/glycerin solutions. After preconditioning was complete, the sets were placed into aging at 77, 120, or 140°F, and at the same relative humidity at which they were preconditioned.

Truncated JANNAF Class C specimens were stamped from the aged slices, then preconditioned for 2 weeks at 45%RH and 77°F. Aluminum end tabs were bonded to the dogbones for testing. Propellant aging was monitored by measuring uniaxial tensile properties at 2 in/min, 77°F, and ambient pressure. A limited number of aging pulls also included 50 in/min, 40°F, and 1000 psig testing, and 2 in/min dilatation testing. Calculation of rate constants was limited to the unpressurized data.

RESULTS AND DISCUSSION

The 2 in/min data were normalized to zero-time properties. Figure 3 shows the aging curves at 140°F. Individual measurements are shown, and the lines simply connect the averages. The solid line connects the average of the 0%RH curve, while the dotted line connects the average of the 5%RH through 25%RH data.

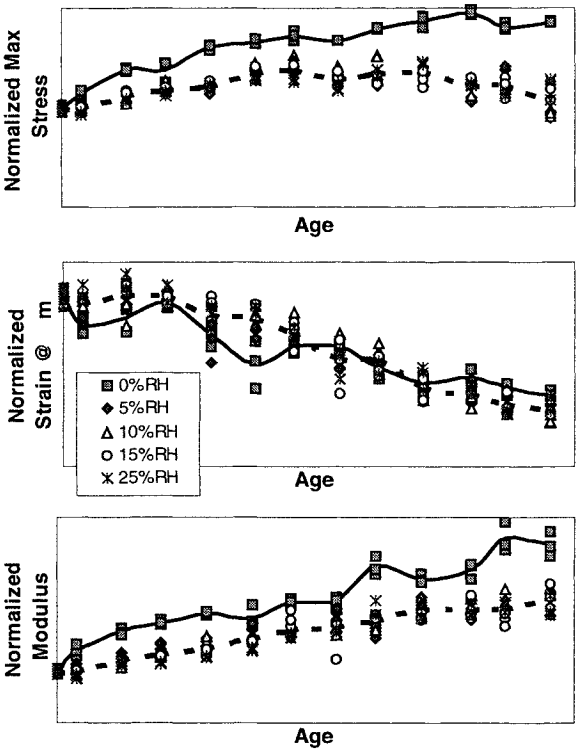

Figure 3. 140°F Propellant Aging Curves

Several observations can be made from the curves shown in Figure 3. There is clear evidence

of hardening with time. Max stress and modulus increase, and strain at max stress decreases. The effect of relative humidity can also be seen. The 0%RH max stress and modulus curves are clearly separated from the rest of the data, and the relative humidity curves roll over as expected for a parallel process aging mechanism. However, in spite of the fact that the 0%RH aging curve is clearly separated from the remaining curves, there is no other obvious effect with respect to relative humidity level. The samples aged at 5%RH through 25%RH appear to form one population. Because of this, the data from samples aged with moisture exposure were handled together as a single set.

Strain at max stress does not show the same kind of aging behavior. The effect of relative humidity apparent in the max stress and modulus aging curves simply does not show up in the strain aging curves. Strain looks nearly unaffected by relative humidity during aging. There does seem to be a very subtle effect however. This can be seen in Figure 4, which shows normalized strain as a function of aging time for both 120°F and 140°F. Only the 0%RH and 25%RH curves are shown, for clarity.

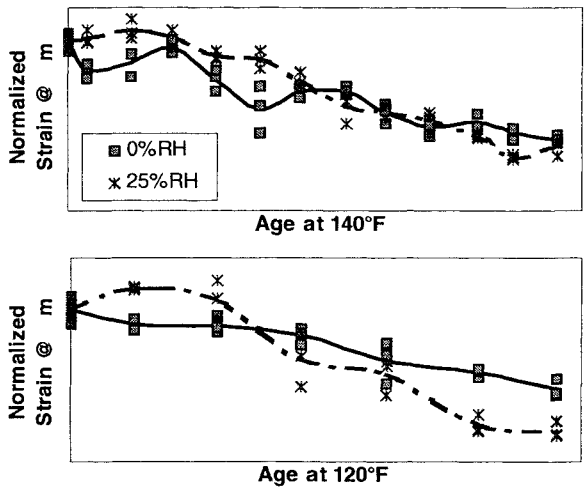

Figure 4. Comparison of Strain Aging Curves

The 0%RH curves show strain steadily decreasing, at least within the limits of the scatter in the data. The 25%RH curves show slightly more complex behavior. Both the 120°F and 140°F 25%RH curves show strain increasing initially, reaching a maximum value, and then decreasing through the remaining aging time. The significance of this behavior is not clear, and even with the slight difference, overall strain aging appears relatively insensitive to the presence or absence of atmospheric moisture.

Figure 5 shows the 140°F aging curves from the limited ignition testing that was done. Only one replicate was tested at each pull, and the data have been normalized to the zero-time test. Although there is some hardening evident in the data, only max stress seems to be strongly affected by the lack of relative humidity. The same difference between the 0%RH and 5-25%RH curves appears in the ignition max stress, but to a lesser extent. Modulus and strain do not show the effect of relative humidity to any appreciable degree.

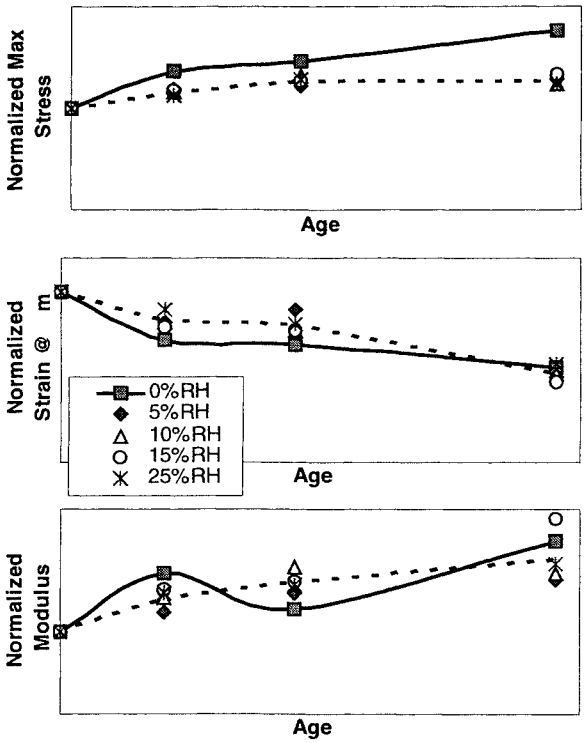

Figure 5. 140°F Ignition Aging Curves

The relative changes in properties with age between the thermal and ignition conditions were also compared. Because there is essentially no aging after nearly two years at 77°F, the thermal and ignition curves were nearly identical. Differences did emerge at the higher aging temperatures, however. At 120 and 140°F, ignition strain showed slightly less relative change than the 2 ipm strain, although the differences that did appear might be the result of scatter in the data. Max stress and modulus showed definite differences; ignition properties showed less relative change with age than the 2 ipm properties.

Ignition properties also showed significantly less sensitivity to relative humidity level.

In addition to the 2 ipm and 50 ipm tests, selected 140°F/25%RH pulls also included uniaxial tensile dilatation tests. These tests were performed at 2 in/min, 77°F, and ambient pressure. Figure 6 shows the stress/strain and volume dilatation curves measured during the course of 140/25%RH aging. Dilatation properties were not measured for any other aging condition.

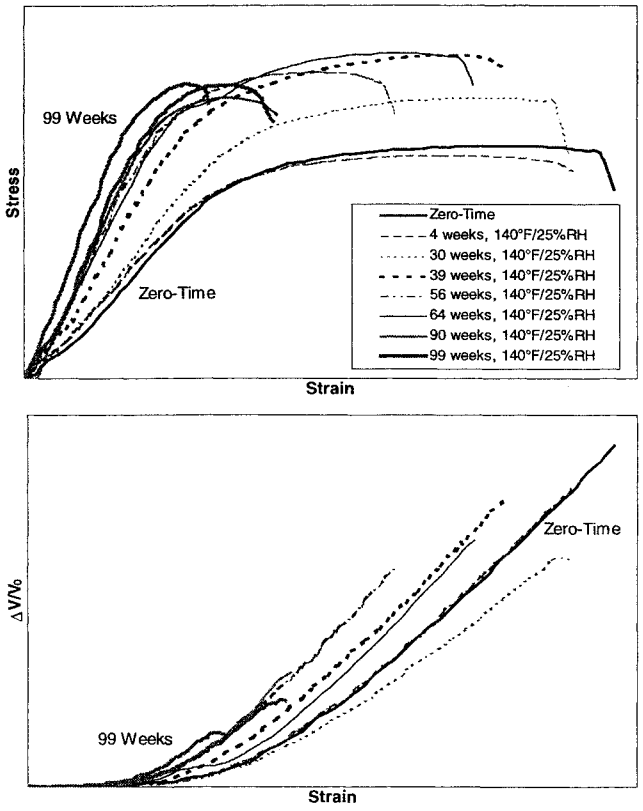

Figure 6. Uniaxial Tensile Dilatation Curves

The stress/strain curves shown in Figure 6 illustrate the changes that occur during 140°F aging clearly. The increase in modulus is easy to see, and the loss of strain is dramatic. Most of the loss in strain occurs in the portion of the stress/strain curve after yield. The volume/strain curves also show large age-related changes, some of which appear to be related to the loss of strain capability. Overall dilatation decreases with age, and the strain at which dilatation occurs also decreases with age.

The dilatation data were analyzed based on the methods developed by R. J. Farris[5]. The volume change that occurs at the onset of deformation (the initial linear portion of the volume/strain curve) is the result of vacuole growth from any pre-existing micro-voids or dewetted solids. This growth continues until active solids dewetting begins, and the curve deviates from the initial slope. Once particle dewetting is complete, the volume/strain curve enters a second linear portion of vacuole growth, which continues until the sample fails. This is shown in Figure 7.

In addition to the qualitative description of a general volume/dilatation curve, Figure 7 also includes a summary of the method used to reduce the data to obtain dilatation properties. Those properties include the total dilatation (the point in the curve where sample failure occurs), the volume fraction of dewetted solids, and the stress and strain of dewetting.

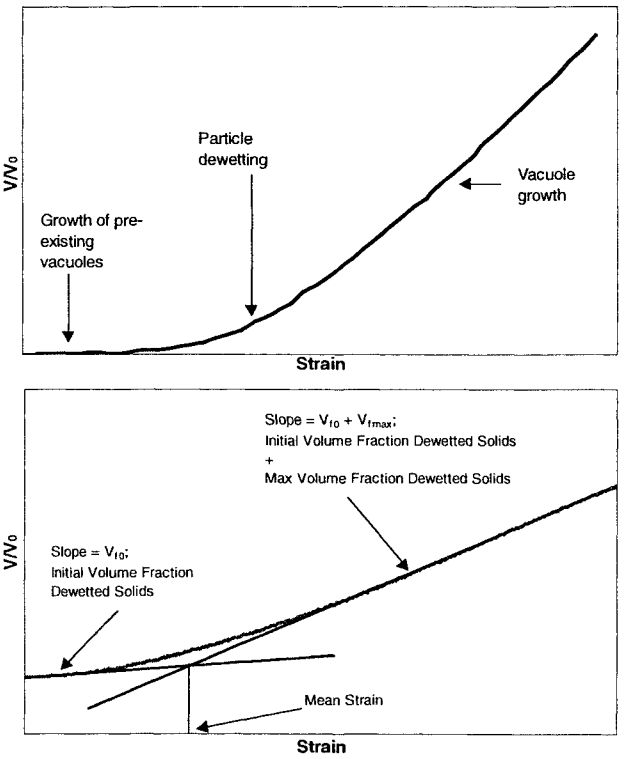

Figure 7. Uniaxial Tensile Dilatation Curves

Figure 8 shows the changes in V_{fmax} and total dilatation with age at 140°F/25%RH. V_{fmax} is the volume fraction of dewetted particles, and total dilatation is the total volume change of the sample during the test. Figure 8 shows total volume dilatation decreases with age. Unlike total dilatation, the volume fraction of dewetted particles does not change significantly with age. Taken together, the data shown in Figure 8 suggest that the decrease in total dilatation with age is due to

the loss of strain capability of the binder, as opposed to a reduction in the amount of dewetting that occurs during deformation.

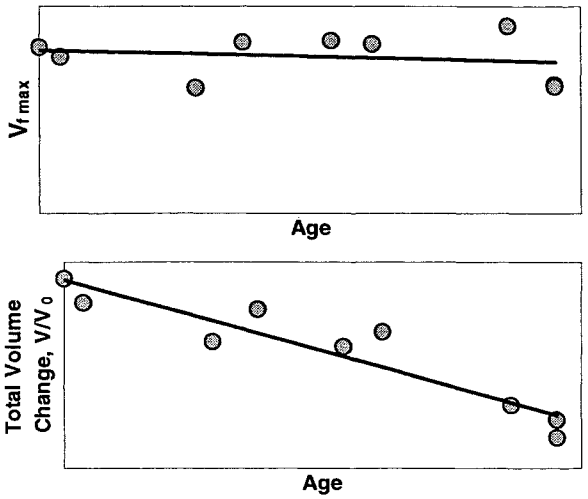

Figure 8. V_{fmax}, and Dilatation Aging Curves

In addition to the dilatation parameters shown in Figure 8, dewetting stress and strain were also calculated. Dewetting strain was expressed as mean strain, defined as the strain at which half of the particle dewetting has occurred. Dewetting stress was determined by using the stress/strain curves (see Figure 6) to pick the corresponding stress at mean strain. Figure 9 shows the dewetting stress and strain as a function of age.

Figure 9 shows mean strain decreases with age. It is possible that the decrease is the result of the increase in modulus that occurs. In other words, because the binder modulus increases with age, the stress required to break binder/filler bonds occurs at lower and lower strains. This explanation requires the corresponding stress be relatively constant with age, which is not the case. It is clear that as mean strain decreases with age, the stress at mean strain increases.

In order to understand the data shown in Figure 9, it is necessary to consider the behavior of dewetting energy. It is possible to generate a rough estimate of the strain energy required for dewetting by simply taking the product of mean strain and its corresponding stress. Figure 9 shows the stress/strain product, plotted as a function of age. The results show the stress/strain product is reasonably constant throughout the bulk of sample aging. There is an indication that the final two pulls are significantly lower than earlier data. For this reason, the final pull was not included in the linear fit shown with the data. This apparent decrease may indicate the beginning of significant changes in dewetting behavior, but the remaining data show very little change with age.

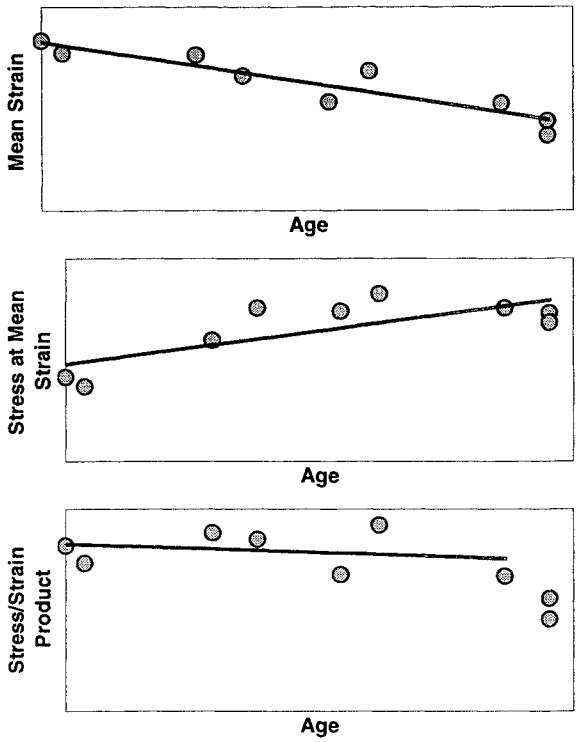

Figure 9. Dewetting as a Function of Age

Taken as a whole, the uniaxial tensile/dilatation results indicate that changes in dilatation involve changes in the polymer network only, and not in binder/filler interactions. The volume fraction of dewetted particles does not change with age. Total dilatation decreases with age, but that appears to be a function of the strain capability of the polymer network. The sample fails earlier in the test, and so vacuoles do not have as much time to grow and contribute to dilatation. Although dewetting strain decreases with age, stress at mean strain increases, and the stress/strain product suggests that particle dewetting is not affected through most of aging.

In addition to the mechanical and dilatation properties, there is additional information available from previous aging studies conducted with the same propellant formulation. These results involve crosslink density/gel measurements made on propellant samples aged at 0%RH as compared to samples aged at 25%RH. The crosslink density/gel measurements were made

using a solvent swell technique. The data are shown in Figure 10, as gel plotted as a function of the corresponding crosslink density.

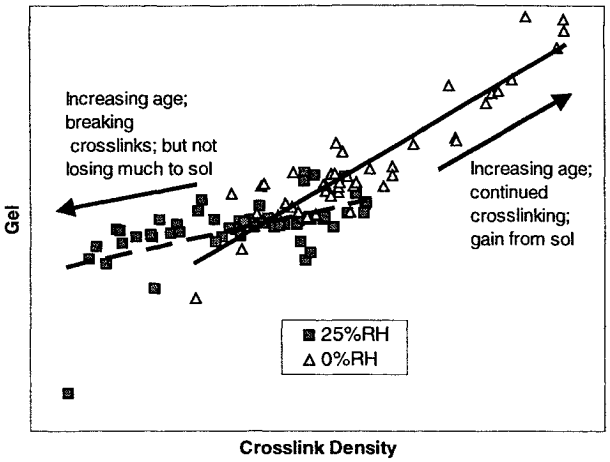

Figure 10. Crosslink Density Vs. Gel

The crosslink density data are shown in this form as a convenient way to gain qualitative mechanistic information. This can be done by examining the way in which the two parameters change with age, relative to each other. It is also a convenient way to look for sub-populations within a set of data, and that is in fact what Figure 10 shows. The samples aged at 0%RH form a distinctly different population from the samples aged at 25%RH.

In this case, the difference between the two populations is related to moisture content and consequent hydrolysis. The aging mechanism for the 0%RH sample population is dominated by oxidative hardening. On the other hand, the aging mechanism for the 25%RH includes a significant degree of hydrolysis, as well as oxidative hardening. The fact that exposure to moisture during aging shows up in crosslink density/gel measurements is an indication that moisture affects the polymer network, as opposed to binder/filler interactions.

It is interesting to note that the three sets of data discussed above, the volume dilatation data, the uniaxial tensile data, and the crosslink density data, are not consistent with each other with respect to the role of relative humidity in composite propellant aging. The uniaxial tensile data show modulus and max stress affected by exposure to relative humidity during aging, but strain shows little change. This strongly suggests that moisture exposure does not affect the HTPB binder network, which implies that it affects binder/filler interactions.

The behavior of the ignition data is also consistent with the idea that moisture affects binder/filler interactions during propellant aging. Superimposed pressure significantly reduces dilatation processes during deformation. This implies anything affecting binder/filler interactions should be less noticeable under ignition conditions. Assuming relative humidity affects the dilatation, then the ignition data should show less sensitivity to moisture, which is what the data show.

However the dilatation data show clearly that dilatation does not change with age at 140°F/25%RH. This indicates moisture aging does not involve binder/solids interactions, suggesting moisture aging primarily involves the polymer network. This is also consistent with the crosslink density data, which shows moisture measurably affects the polymer network during aging.

One possible explanation for the contradiction that exists in the data involves the bonding agent used to provide a 'link' between the solid filler and the polymeric network. In the case of this particular propellant formulation, the bonding agent is an epoxy-amine system. There is evidence that the epoxy does not actually participate in forming the link between the solid filler and HTPB, so the remaining discussion will focus on the role of the amine.

During propellant manufacture, the amine portion of the bonding agent is added to the propellant prebatch and allowed to react with the oxidizer. The result of the reaction is an ionic bond between the amine and oxidizer particle. In addition a layer of amine bonding agent forms to cover the solid particle.

During the final mix step, some of the isocyanate reactive groups in the crosslinkers react with residual amine groups left in the layer of bonding agent that covers the particle surface. This reaction forms substituted urea groups. During propellant cure, hydroxy groups from the HTPB react with the remaining isocyanate groups bound to the layer of bonding agent, to complete the process of linking the solid particles to the polymer network.

Once cure is complete, the propellant essentially consists of solid particles covered with a layer of non-rigid bonding agent, embedded in a polymer matrix. The right-hand sketch of Figure 11 shows

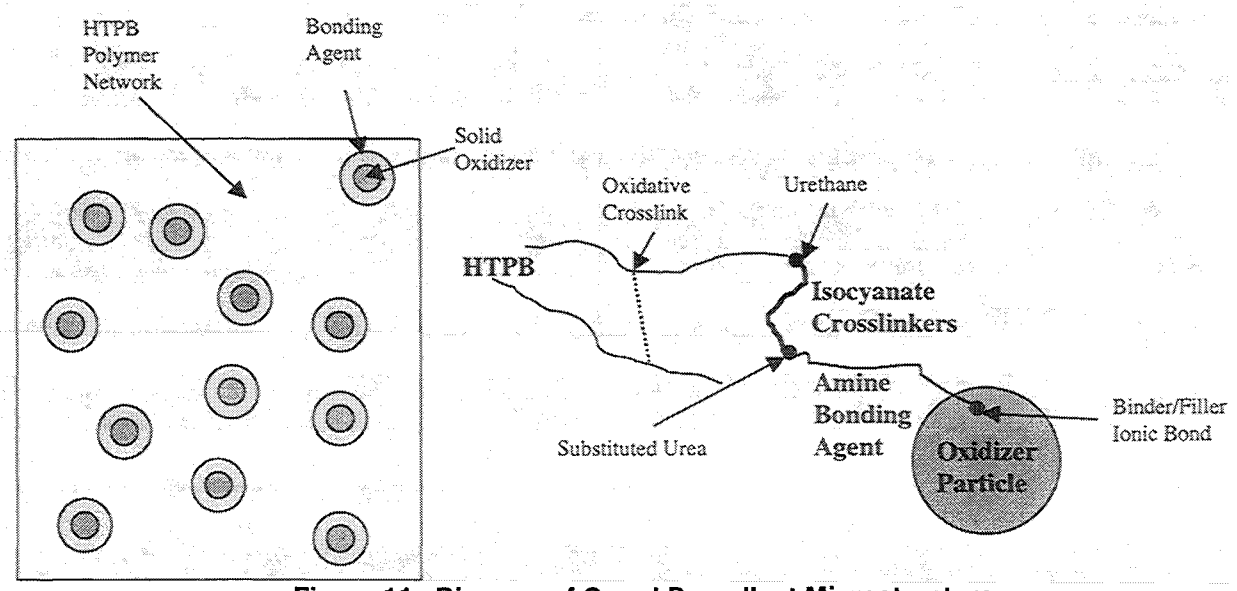

Figure 11. Diagram of Cured Propellant Microstructure

a rough schematic of the chemical bonds that form between the solid oxidizer particles and the polymer network. The left hand sketch shows the resulting propellant microstructure.

Clearly the hardening that occurs during composite propellant aging is the result of oxidative crosslinking at the double bonds in the HTPB polymer network. This is well known for polybutadiene networks, and is the reason for the standard addition of anti-oxidants.

However, the role of water is not clear. It is reasonable to assume water would attack the ionic binder/filler bond, but the dilatation data clearly show that this does not occur. Perhaps the layer of bonding agent covering the particle surface protects the binder/filler bonds from moisture attack. It is also possible that the decrease in the stress/strain product at the very end of 140°F aging (see Figure 9) is the first indication of moisture attack at the ionic bond. It may simply take time for the water to diffuse through the polymer network and then through the layer of bonding agent.

There are only two other possible sites for hydrolytic attack, the urethane bond that forms the polymer network, and the substituted ureas that form between the amine bonding agent and the isocyanate crosslinkers. It is unlikely that moisture affects the urethane bonds. They are very stable chemically, and are not typically subject to hydrolytic attack. In addition, the mechanical property data show that this does not occur. The fact that strain aging is not affected by exposure to relative humidity strongly suggests there is no hydrolytic attack of the urethanes that form the HTPB polymer network.

This leaves the substituted urea, which can be subject to hydrolytic attack. Assuming this mechanism, moisture attack of the substituted urea groups, it is possible to explain the apparent contradictions in the data, at least to some degree. Given the fact that modulus is a function of both binder stiffness and binder/filler interactions, it is reasonable to assume that modulus would also be affected by anything in between, such as the bonding agent layer on the solid particle surface.

Stress is also a function of both binder stiffness and binder/filler interactions. And in spite of the fact that aging in the presence of relative humidity does not directly affect binder/filler interactions, attack of the substituted urea groups will change the way the load is distributed during deformation. Changes in the way the microstructure distributes load will certainly affect measured stress.

On the other hand, strain is driven almost exclusively by the properties of the binder network. There is no contribution from binder/filler interactions. Although the bonding agent layer might have some effect on strain, that effect will probably be minor, since the bonding agent is not an integral part of the HTPB polymer network. The amine bonding agent is on the periphery of

the overall propellant polymer network, instead of being fully incorporated into it.

Finally, hydrolytic attack of substituted urea groups is also consistent with the crosslink density data (see Figure 10). The bonding agent is chemically bound to the polymer network. It will contribute to the way in which the network behaves during a solvent swell test. Changes to the bonding agent during the course of aging will be reflected in crosslink density.

The chemical mechanism discussed above was used to select the appropriate kinetic models used to fit the mechanical property aging data. Based on this mechanism, two models were chosen. The max stress and modulus data were fit using the parallel process model. Strain was fit using a simple first order (exponential) model. Although moisture does seem to have a subtle effect on strain, an exponential fit was chosen as a reasonable approximation of the overall aging behavior observed.

The data used in the kinetic analysis included the data generated in the study discussed above, and data from an earlier study with which this one was designed to merge. The parallel process model was fit to the stress and modulus data in the following manner:

1. Since the properties were normalized to zero-time measurements to remove mix-to-mix variability, P_0, was set equal to one, and held constant for all subsequent model fits.
2. The parameter F, related to the maximum fractional increase of the property of interest, was determined visually, and held constant over all aging conditions (temperature and relative humidity).
3. Samples aged with moisture exposure (i.e., 5%RH to 25%RH) were considered to form one population, and were not handled separately. The data were averaged together to form one set of aging curves.
4. The oxidative hardening and hydrolysis rate constants were solved for simultaneously using a non-linear regression technique.

Figure 12 shows the Arrhenius curves for the hardening and hydrolysis rate constants calculated for stress and modulus, and the hardening rate constants for strain.

The oxidative rate constants shown in Figure 12 are reasonably well behaved, and appear to be linear. The calculated activation energies for stress, strain, and modulus are very similar, and range between 12 – 14 kcal/mole.

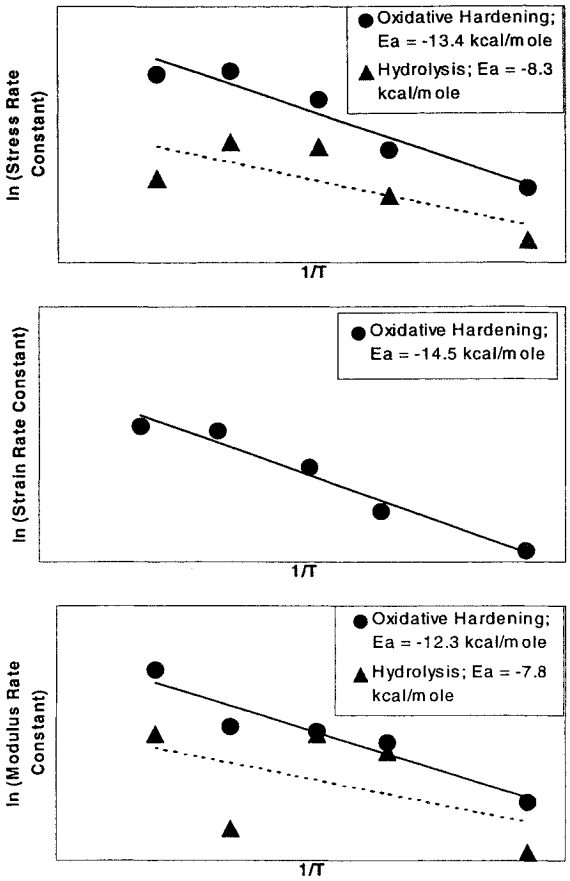

Figure 12. Arrhenius Curves for Oxidative Hardening and Hydrolysis Rate Constants

There is considerably more scatter in the hydrolysis rate constants. This is probably a reflection of the difficulty in applying a four-adjustable-parameter model to the data from the previous study, which had a limited number of observations at any one aging condition. In addition, some scatter is introduced, because for some aging temperatures, the model fit was forced to 'average' over two sets of data, from the current study and the previous study. This has the effect of making some of the calculated rate constants more 'average' than others, depending on whether or not data from both studies were available at any given aging temperature.

In spite of the scatter in the hydrolysis rate constants, the activation energies calculated are very similar for stress and modulus, on the order of 8 kcal/mole. An activation energy of this

magnitude suggests the hydrolysis reaction could be diffusion limited.

Figure 13 shows ambient aging data from both aging studies, spanning a total of ten years. The data are from samples aged in the presence of moisture, ranging from 5%RH to 25 %RH. The bulk of the data were aged using an as-built relative humidity. The kinetic model fits; parallel process for stress and modulus, first order for strain, are included. In spite of the scatter in the data, particularly in the modulus values (not unusual for composite propellant aging), the models fit the data well.

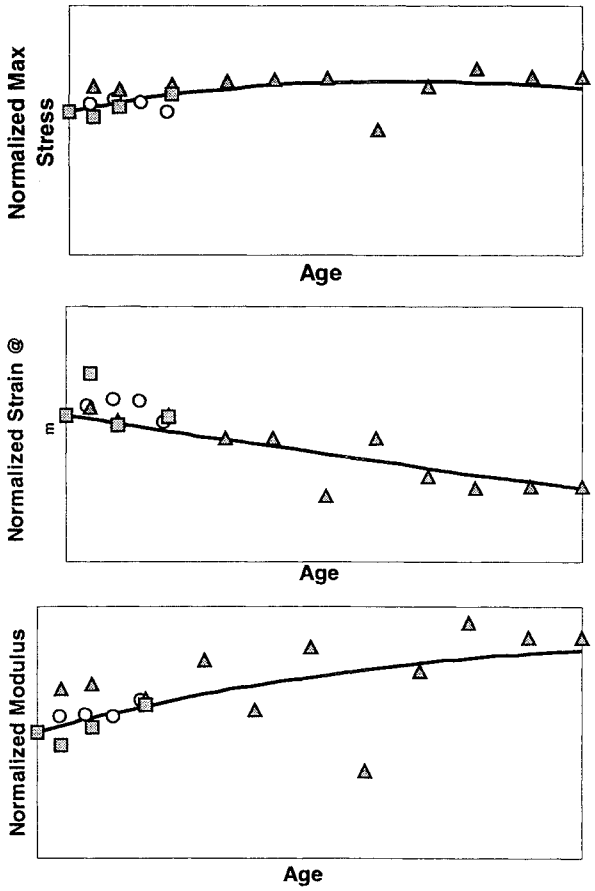

Figure 13. Model Fit of Ambient Aging Data

In addition to the sub-scale aging data shown in Figure 13, there are data available from full-scale motors. These motors have been aged under ambient conditions and motor plugs containing propellant and case bond periodically removed and characterized. It is possible to compare the model fits to data from these full-scale motor plugs. This was done by vertically shifting the 77°F model curves, until a best fit with the plug data was achieved.

Although the motor plug data did not include zero-time data, it was possible to evaluate the model fit not only by the agreement of the curve with the actual data, but also by the magnitude of the zero-time values predicted by the model. The results of a comparison with 2 in/min/77°F/0 psig mid-web propellant data are shown in Figure 14.

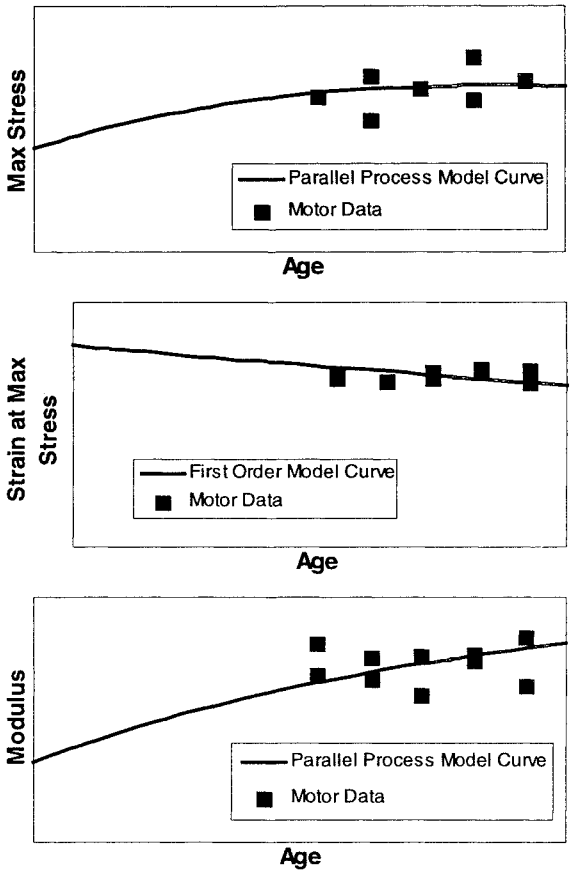

Figure 14. Comparison of 77°F Model Curves to Motor Plug Data

Overall, Figure 14 shows that the parallel process model over-predicts the degree of aging that occurs, particularly for modulus. Although the agreement between the model curve and the data is reasonable for both stress and strain, the comparison is poor for modulus. In addition, the extrapolated zero-time values for all three properties are lower than what might reasonably be expected for motor mid-web propellant.

The fact that the model over-predicts mid-web propellant is not surprising, and is consistent with what might be expected based on the description of propellant aging given earlier. The plug data are from mid-web propellant that has seen no

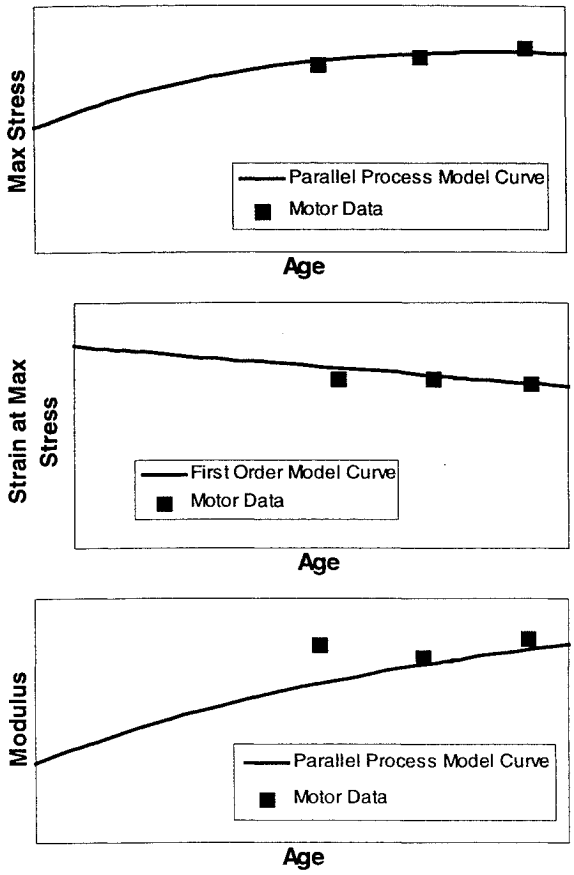

Figure 15. Comparison of Model Curves to Motor Plug Data – Restricted to One Mix

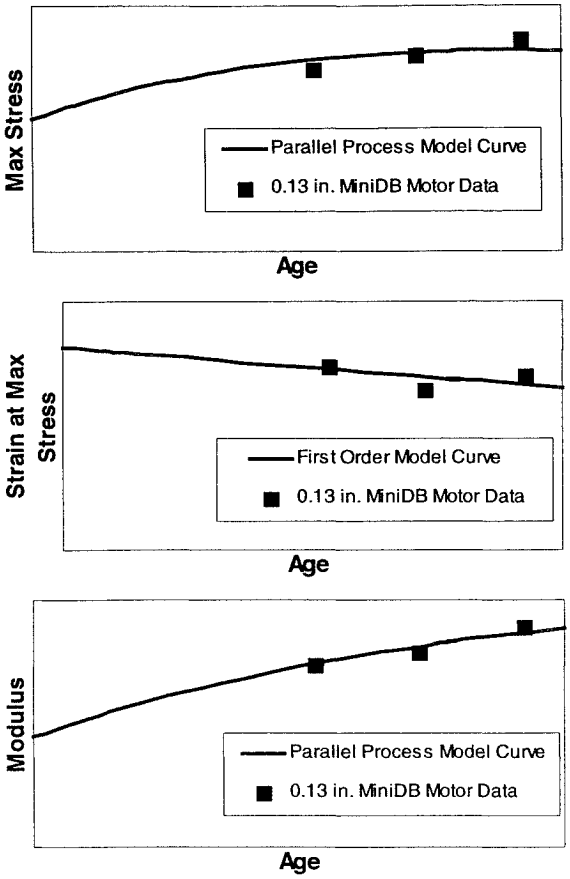

Figure 16. Comparison of 77°F Model Curves to Motor Bore Propellant Profile Data

atmospheric exposure during aging, while the model was developed using samples that saw substantial atmospheric exposure. Since the degree of aging that occurs is driven by the diffusion of oxygen and water, samples that represent near-surface propellant should show greater aging than mid-web samples.

In addition to the differences in atmospheric exposure there are other sources for the differences between motor data and the model curves. There are two motors, with at least four different full-scale mixes represented in the plug data. Finally, the motor properties were generated using non-truncated JANNAF Class C dogbones, while the model was developed from properties measured with truncated JANNAF Class C dogbones. There is a bias between the two test specimen configurations, which may not be constant with age.

Figure 15 shows the same comparison of model curves to motor plug data, with the motor data restricted to a single motor and a single mix. This reduces the amount of motor data available for the comparison to three points. Restricting the data to a single mix does improve the agreement between the model curves and motor data slightly. The models still over-predict the amount of aging that occurs, particularly for modulus. However, the extrapolated zero-time properties increase slightly when based on a single mix. They are still low, but are closer to reasonable values.

In addition to mid-web propellant properties, the motor plug testing also included mechanical property profiles of bore propellant. The data from the near-surface samples were compared to the model curves, in the same manner as the mid-web propellant properties. The model curves were shifted vertically until a best fit with the data was achieved. The motor near surface profile data were also restricted to a single motor and single mix, the same motor and mix shown in Figure 15. The results of the comparison are shown in Figure 16.

The agreement between model curves and near-surface propellant properties is excellent, even in terms of modulus. The curves follow the data very well. In addition, the extrapolated zero-time properties from each model curve are very reasonable. Overall, the models used to describe the aging data compare very well with actual aged motor data, particularly near-surface propellant.

REFERENCES

1. SDRL SR-T01; Report for Titan IV SRMU Enhanced Aging and Surveillance; Nov 2000.

2. M. Celina, A. C. Graham, K. T. Gillen, R. A. Assink, L. M. Minier; "Thermal Degradation Studies of a Polyurethane Binder"; 156th Meeting of the Rubber Division, ACS; Orlando, Florida; Sept 21 – 24 1999; Paper # 66.

3. R. L. Kelley; *"Parallel Processes Kinetic Model"*; JANNAF S&MBS; Oct 1987.

4. K. W. Bills, D. O. DePree, R. K. McCamey, R. M. Smith; *"The Chemical Kinetic Approach to Service Life Prediction of Propellant Systems"*; AIAA/SAE/ASME 15th Joint Propulsion Conference; Las Vegas NV; June 1979.

5. R. J. Farris; CPIA Publication 61U, Vol I, 1964.